Molecular dynamics simulations of strongly coupled plasmas

2009 J. Phys. A: Math. Theor. 42 214029

(http://iopscience.iop.org/1751-8121/42/21/214029)

IOP PUBLISHING JOURNAL OF PHYSICS A: MATHEMATICAL AND THEORETICAL

J. Phys. A: Math. Theor. **42** (2009) 214029 (13pp) doi:10.1088/1751-8113/42/21/214029

Molecular dynamics simulations of strongly coupled plasmas

Z Donkó

Research Institute for Solid State Physics and Optics, Hungarian Academy of Sciences, POB 49, H-1525 Budapest, Hungary
and
Department of Physics, Boston College, Chestnut Hill, MA 02467, USA

E-mail: donko@mail.kfki.hu

Received 29 September 2008, in final form 20 November 2008
Published 8 May 2009
Online at stacks.iop.org/JPhysA/42/214029

Abstract

Computer simulation methods represent a complementary approach to experimental and theoretical studies, and they have become invaluable tools for the description of many-particle systems in numerous disciplines of science. One of the main and widely applied approaches is the molecular dynamics simulation, which makes it possible to trace the phase-space trajectories of particles thereby providing information about the time evolution of the systems investigated. From the phase-space coordinates of the particles, it is possible to derive static, thermodynamic as well as transport properties and to obtain information about the collective excitations.

PACS numbers: 52.27.Gr, 52.27.Lw, 52.65.Yy

1. Introduction

Strongly coupled plasmas (SCPs)—in which the average potential energy per particle dominates over the average kinetic energy—appear in a number of physical systems: dusty plasmas, charged particles in cryogenic traps, condensed matter systems such as molten salts and liquid metals, electrons trapped on the surface of liquid helium, astrophysical systems, such as the ion liquids in white dwarf interiors, neutron star crusts, supernova cores and giant planetary interiors, as well as degenerate electron or hole liquids in two-dimensional or layered semiconductor nanostructures. These systems and a wide variety of phenomena taking place in them have been covered by the *Strongly Coupled Coulomb Systems* conference series [1].

This paper intends (i) to review the utilization of molecular dynamics (MD) simulations in the determination of prominent characteristics of some types of SCPs and (ii) to discuss some open problems of the field. It is of course impossible to consider here all types of SCPs, which can be divided into several categories according to their chief characteristics:

their composition, spatial dimensionality, spatial extent and configuration, and classical versus quantum behavior.

Regarding their composition, SCPs may consist of a single or multiple types of charged species. As an example of a single-component system, the layer of electrons on the surface of liquid helium [2, 3] may be mentioned. Neutron star crusts are composed of fully stripped iron ions; in the core of Jovian planets we find a binary mixture of H^+ and He^{2+} ions [4], while the core of white dwarf stars consists of a mixture of fully stripped ions of C, N and O [5]. In these systems, electrons are present as a neutralizing background. Dusty plasmas, in addition to electrons and ions, contain mesoscopic dust grains, which charge up and respond to electromagnetic fields [6].

Regarding dimensionality and spatial extent, the above-mentioned astrophysical objects are usually modeled as infinite three-dimensional (3D) systems. In laboratory studies, two-dimensional (2D) and one-dimensional (1D) settings (e.g. of charged grains levitated in low pressure gas discharges) have also been extensively studied. Multiple layered configurations can be realized in semiconductor heterostructure devices [7], ion traps [8] and dusty plasma experiments using two different sized grains [9]. Finite 3D and 2D clusters of charged grains have also been realized in gaseous discharges and attract considerable attention lately; see, e.g., [10].

Here we restrict our studies to classical systems which can be described within the framework of the one-component plasma (OCP) model, in which only one of the components of the plasma is considered explicitly, while the presence and effects of other types of species are accounted for by the interparticle potential. In the OCP model, for Coulomb and Yukawa plasmas, respectively, the potentials

$$\phi(r) = \frac{Q}{4\pi\varepsilon_0}\frac{1}{r} \tag{1}$$

and

$$\phi(r) = \frac{Q}{4\pi\varepsilon_0}\frac{\exp(-r/\lambda_D)}{r} \tag{2}$$

are applicable. Here, Q is the charge of the particles and λ_D is the Debye length.

The strength of the coupling (related to the ratio of the interparticle potential energy to the kinetic energy per particle) is expressed by the *coupling parameter*:

$$\Gamma = \frac{Q^2}{4\pi\varepsilon_0}\frac{1}{ak_BT}, \tag{3}$$

where a is the Wigner–Seitz (WS) radius and T is the temperature. In the case of Yukawa interaction, an additional essential parameter is the *screening parameter*:

$$\kappa = \frac{a}{\lambda_D}. \tag{4}$$

The strong coupling regime corresponds to $\Gamma > 1$. In the $\kappa \to 0$ limit the interaction reduces to the Coulomb type, while at $\kappa \to \infty$ it approximates the properties of hard spheres.

SCPs, seen as many-particle systems, can be treated theoretically in a straightforward way in the limits of both weak interaction and very strong interaction. In the first case, one is faced with a gaseous system, where correlation effects can be treated perturbatively. In the case of very strong interaction, the system crystallizes and phonons are the principal excitations. In the intermediate regime—in the *strongly coupled liquid phase* [11]—the localization of the particles in the local minima of the potential surface still prevails; however, due to the diffusion of the particles, the time of localization is finite [12]. The strongly coupled liquid phase is the very domain where computer simulations have proven to be invaluable tools. Among the fields

of theory, experiment and simulations, the latter has experienced the most dramatic advance of resources during the past few decades. In the pioneering studies of the 1960s and 1970s, systems consisting of few hundred particles were possible to simulate. Recently, simulations of $\sim 10^3$–10^6 particles (depending on the type of potential) can be considered as standards; the largest supercomputers allow this number to grow to $\sim 10^9$ [13]. With the rapid development of computational tools, an even more extensive use of simulation techniques is expected in the future.

The paper is organized as follows. Section 2 gives a brief description of the MD simulation technique. In sections 3–5 representative examples of results obtained by MD simulations are presented, respectively, for static properties, collective excitations and transport properties of SCPs. The summary is given in section 6.

2. Molecular dynamics simulations

Molecular dynamics simulations follow the motion of particles by integrating their equations of motion while accounting for the pairwise interaction of the particles, as well as for the forces originating from any external field(s); see, e.g., [14]. The 'core' of the MD codes describes the time evolution of phase-space trajectories of the ensemble of particles, while 'measurements' implemented in the code provide information (from the phase-space coordinates) about the quantities of interest: about density and current oscillations, transport coefficients, as well as the pair correlation function, which gives insight into the structure of the systems and is the basis of the calculation of thermodynamic quantities.

The studies presented here concern 'idealized' Coulomb and Yukawa systems, in which the Newtonian equation of motion was assumed to hold. In other words, the friction and random forces originating from the plasma/gas background environment (see e.g. [15]) were not taken into account. Also, all the examples in this paper are given for unconfined systems, for which no external potential is applied and periodic boundary conditions are used.

The calculation of the force acting on a particle of the system is relatively simple in the case of short-range potentials (e.g. Yukawa potential with high κ); in this case, MD methods make use of the truncation of the interaction potential thereby limiting the need for the summation of pairwise interactions around a test particle to a region of a finite size.

In the case of long-range interactions (e.g. Coulomb or low-κ Yukawa potentials), however, such truncation is not allowed, and the periodic images of the system in all principal directions have to be taken into account in the calculation of the interaction forces (see figure 1). In the case of Coulomb interaction, in particular, the summation needs to be extended to infinity in all directions. Convergence problems may be overcome by using special techniques, such as Ewald summation [16], the fast multipole method or the particle–particle particle-mesh (PPPM or P3M) method [17, 18].

In the Ewald summation method [16], the interaction potential is split into two parts, one of which converges rapidly in real space and the other converges rapidly in the Fourier space. This method has been used, e.g., in the calculation of transport coefficients of Yukawa liquids [19] and in simulations of bilayer systems [20].

The PPPM method introduced by Eastwood, Hockney and Lawrence [17] also uses a partitioning of the interaction into (i) a force component that can be calculated on a mesh (the 'mesh force') and (ii) a short-range ('correction') force which is to be applied to closely separated pairs of particles only. In the mesh part of the calculation, charge clouds are used instead of pointlike charges. The charge density distribution is assigned to a grid and is Fourier transformed to the $\mathbf{k}$-space. Mutiplying $\rho(\mathbf{k})$ with an optimized Green function results in a potential distribution $\phi(\mathbf{k}) = G(\mathbf{k})\rho(\mathbf{k})$, which is subsequently transformed back to real

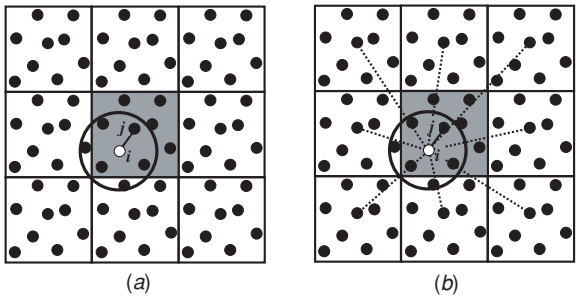

Figure 1. Molecular dynamics simulation using periodic boundary conditions in the case of short-range (*a*) and long-range (*b*) potentials. This illustration is for two dimensions. The shaded region is the primary simulation box. In (*a*), the circle shows the cutoff radius; the particles (one of them is denoted by *j*) interacting with the white test particle *i* have to be searched for inside this domain. In the case of long-range potentials (*b*) interaction with the particles situated in the periodic images of the primary box (up to infinity in all principal directions) must be taken into account. The correction force (see text) is to be applied to closely separated pairs located within a circle.

space. The forces acting on the particles are obtained by differentiation of the potential and interpolating the electric field to the positions of the particles. The cloud shape is chosen in a way to ensure that $\rho(\mathbf{k})$ is band-limited. (This would not be the case with pointlike charges.) The calculation of the potential in the Fourier space automatically takes into account the periodic images of the primary computational cell. For closely separated particles a correction force is to be applied, which is the difference between the forces between two pointlike charges and two charges with the cloud shape used. For more details, see [17].

In our molecular dynamics simulation studies of strongly coupled Coulomb systems we have used the PPPM method, while in the studies of Yukawa systems we have applied the summation of the interaction forces within a finite cutoff radius, the value of which depended on the screening parameter.

3. Static properties and phase transitions

In three dimensions at $\kappa = 0$, the liquid phase is limited to coupling parameter values $\Gamma \leqslant 175$ [21]. A first-order phase transition was identified to take place at $\Gamma \cong 175$, where the plasma is known to crystallize into a *bcc* lattice [22]. We note that at $\kappa > 0$, the 3D systems may crystallize either in a *bcc* or in a *fcc* lattice, depending on the value of κ [23].

At high values of the coupling coefficient, liquid-phase plasmas exhibit strong structural correlations. Such correlations can easily be studied by examining the pair correlation function (PCF, $g(r)$), which also serves as the basis of the calculation of the thermodynamic characteristics of the systems; see, e.g., [24]. Figure 2 shows pair correlation functions for the 3D Coulomb OCP for a series of Γ values. At high Γ, we observe very strong correlation in the particle separations corresponding to those of a *bcc* lattice. With decreasing Γ the peak amplitudes of $g(r)$ decrease, but the positions of the peaks remain nearly unchanged. This remarkable feature of the PCFs indicates that the *local* environment of the particles in the liquid phase still resembles the underlying ($\Gamma \to \infty$) lattice configuration. At high Γ values, the strong correlation arises from the prominent quasilocalization of the particles in the local minima of the potential surface. It has been shown by simulations [12] that the period of localization typically covers several plasma oscillation cycles before particle

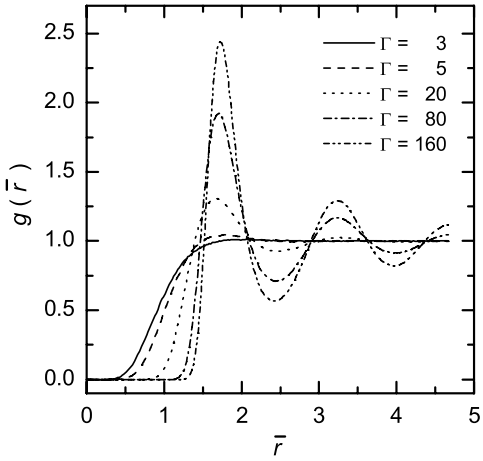

Figure 2. Pair correlation functions of the classical 3D Coulomb OCP, for different values of the coupling parameter Γ. The distance is normalized by the WS radius.

migration rearranges the potential surface. This 'caging' behavior, appearing at high values of Γ, determines many of the systems' properties [25].

Regarding systems with lower dimensionality ($\mathcal{D} < 3$) it has been theoretically shown that exact long-range order cannot survive at finite temperatures $T > 0$, for a potential with $\kappa > 0$ [26]. Thus, infinite (Yukawa) single crystals do not exist in 2D. Nonetheless, crystal-like and fluid-like behavior have been observed in 2D systems and pronounced changes of certain characteristics (e.g. bond angular order parameter) have been detected in the transition region between these two 'phases'; see, e.g., [27]. In many papers on 2D systems (most frequently, 2D dusty plasma configurations), the words 'phase' and 'phase transition' have been routinely used. One should, however, be aware of the above-mentioned arguments against the existence of true long-range order and real phase transitions taking place in low dimensional Yukawa systems.

In two dimensions, crystallization of a Coulomb system into a hexagonal lattice was found to occur at a coupling $\Gamma \approx 137$, as indicated by both experiments [2] and computer simulations [28]. Theoretical (see e.g. [29, 30]) and numerical studies of the 'melting transition' in 2D systems indicate the appearance of two melting stages. According to this theory, as the system is heated it first transforms from a solid into a 'hexatic' phase, where the quasi-long-range positional order is suppressed, but the orientational order still survives. At somewhat higher temperatures, the orientational order also disappears and the system enters the liquid phase. This issue of the number of distinct phases in 2D Coulomb or Yukawa systems has been, for some time, a matter of intense controversy [31]. As an example of studies where two-stage melting was found to occur, [32] may be mentioned. The increasing interest in finite (classical and quantum) systems (sometimes consisting of a few particles only) has motivated studies of the transition between solid-like and liquid-like phases [33].

4. Collective excitations

Collective excitations (waves) are prominent features of plasmas. Depending on the dimensionality and the confinement of the system, different collective excitations (longitudinal

and transverse modes) appear. The spectrum of density fluctuations (the dynamical structure function) is calculated as [34]

$$S(k,\omega) = \frac{1}{2\pi N}\int_{-\infty}^{\infty} \mathrm{e}^{\mathrm{i}\omega t}\langle\rho(k,t)\rho(-k,0)\rangle\,\mathrm{d}t$$
$$= \frac{1}{2\pi N}\lim_{\Delta T\to\infty}\frac{1}{\Delta T}|\rho(k,\omega)|^2, \tag{5}$$

where N is the number of particles and $\rho(k,\omega)$ is the Fourier transform of the microscopic density:

$$\rho(k,t) = \sum_j \exp[\mathrm{i}kx_j(t)]. \tag{6}$$

The $(1/\Delta T)$ factor in (5) enters because in the calculation of the $\langle\rho(k,t)\rho(-k,0)\rangle$ autocorrelation function, the ensemble average is replaced by the time average (assuming ergodicity)

$$\langle\rho(k,t)\rho(-k,0)\rangle = \frac{1}{\Delta T}\lim_{\Delta T\to\infty}\int_0^{\Delta T}\rho(k,t+t')\rho(-k,t')\,\mathrm{d}t'. \tag{7}$$

Similarly, the spectra of the longitudinal and transverse current fluctuations, $L(k,\omega)$ and $T(k,\omega)$, respectively, can be obtained from the Fourier analysis of the microscopic quantities:

$$\lambda(k,t) = k\sum_j v_{jx}(t)\exp[\mathrm{i}kx_j(t)], \tag{8}$$

$$\tau(k,t) = k\sum_j v_{jy}(t)\exp[\mathrm{i}kx_j(t)], \tag{9}$$

where x_j and v_j are the position and velocity of the jth particle, respectively. Here, we assume that $\mathbf{k}$ is directed along the x-axis (the system is isotropic) and accordingly omit the vector notation of the wave number. The above-described way for the derivation of the spectra provides information for a series of wave numbers, which are multiples of $k_{\min} = 2\pi/H$, where H is the edge length of the simulation box.

Longitudinal modes can fully be characterized by the dynamical structure function $S(k,\omega)$, while transverse modes can be studied through the analysis of the transverse current fluctuation spectra $T(k,\omega)$. The corresponding current fluctuation spectra for the longitudinal mode, $L(k,\omega)$, are linked with the dynamical structure function. Collective excitations are identified as peaks in these MD-generated spectra, and dispersion relations are derived by observing the change of the frequency (where the peaks are found) with the wave number. Additionally, the widths of the peaks in the spectra convey information about the lifetime of excitations (associated with the damping of the waves), as well as about the distribution of the mode frequencies due to the disordered particle configuration in the liquid phase.

Molecular dynamics simulations have been used in studies of collective excitations in Coulomb [34] and Yukawa [35, 36] plasma liquids. In the following, as an example, we present MD simulation results for the collective excitations in 3D Coulomb and Yukawa liquids, and compare these with the predictions of the quasilocalized charge approximation (QLCA) theory.

Longitudinal ($L(k,\omega)$) and transverse ($T(k,\omega)$) current fluctuation spectra are plotted in figure 3 for wave numbers, which are multiples of $\bar{k}_{\min} = k_{\min}a = 0.167$. $L(k,\omega)$ obtained for the Coulomb case ($\Gamma = 160$, $\kappa = 0$) peaks very nearly at the plasma frequency ω_0. In the case of the Yukawa potential, as shown in figure 3(b), the behavior of $L(k,\omega)$ changes significantly:

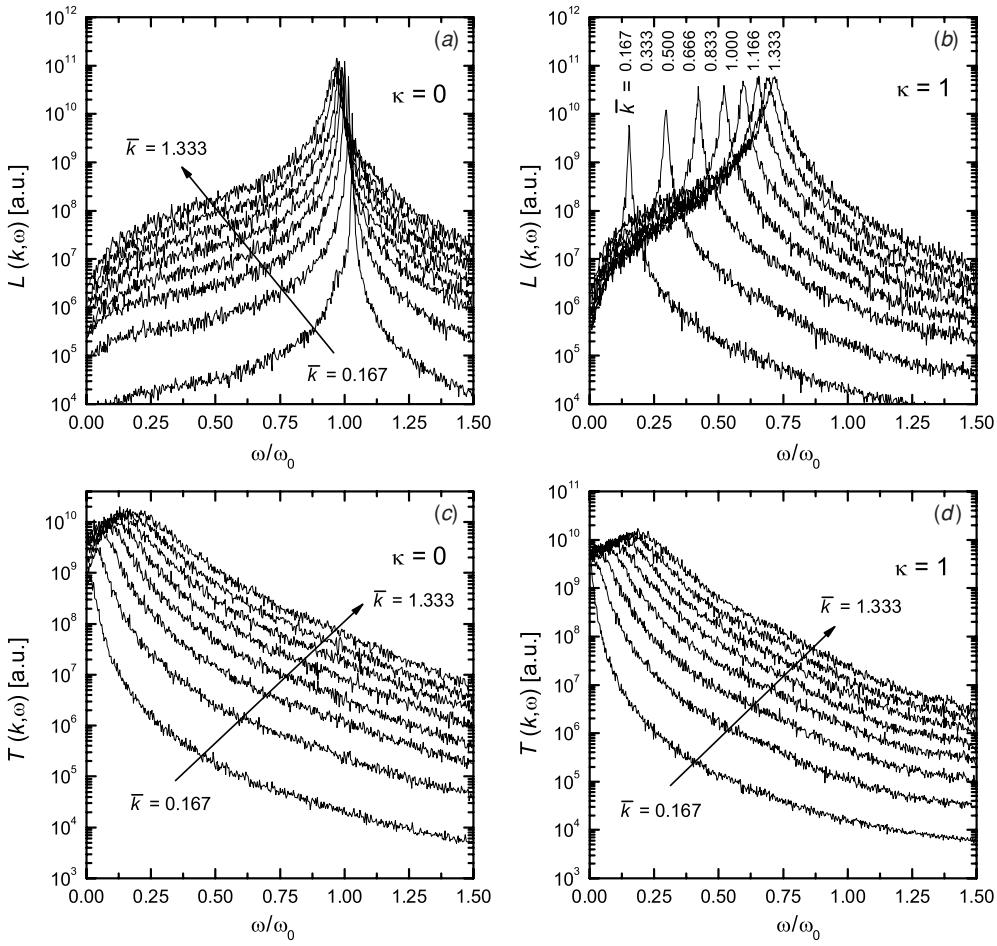

Figure 3. Longitudinal current fluctuation spectra in a 3D Coulomb OCP at $\Gamma = 160$ (*a*) and in a Yukawa OCP at $\Gamma = 200$, $\kappa = 1$ (*b*). Transverse current fluctuation spectra for the same parameter values (*c*), (*d*). $\bar{k} = ka$ denotes the dimensionless wave number; its values are given in (*b*). In (*a*), (*c*), (*d*), the arrows indicate increasing values of $\bar{k}$. The number of particles in the simulation: $N = 12\,800$. Partly reproduced from [11] (copyright (2008) by IOP Publishing).

at $\bar{k} \to 0$ the wave frequency $\omega \to 0$. The contrast between the $\kappa = 0$ and the $\kappa > 0$ cases is also well seen in figure 4, where the dispersion curves derived from the fluctuation spectra are displayed. The (Γ, κ) pairs for which the dispersion graphs are plotted in figure 4 have been selected to represent a constant 'effective' coupling $\Gamma^* = 160$. This definition of Γ^* relies on the constancy of the first peak amplitude of the pair correlation function $g(\bar{r})$, similar to the case of 2D Yukawa liquids [37].

Compared to those characterizing the $\mathcal{L}$ mode, peaks in the $\mathcal{T}$ mode spectra are rather broad, as can be seen in figures 3(*c*) and (*d*), for the Coulomb and Yukawa cases, respectively. In the case of this mode, there is no significant change between the behavior when κ changes from a zero to a nonzero value; only the mode frequency decreases, as can also be observed in figure 4(*b*).

A comparison of the dispersion relations obtained from the MD and those from the QLCA theory [11, 38] is presented in figure 4. The agreement between the dispersion curves

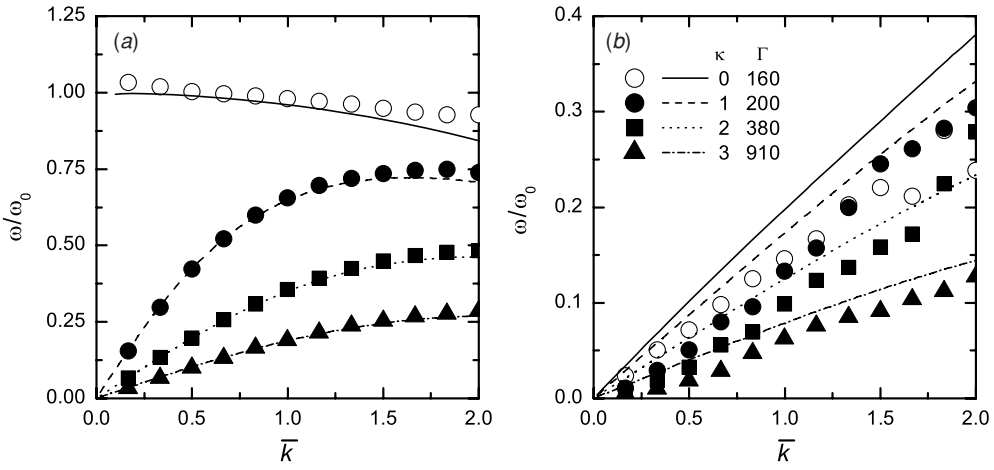

Figure 4. Dispersion relations for the (*a*) longitudinal and (*b*) transverse modes of 3D Coulomb and Yukawa plasma liquids. Symbols represent molecular dynamics results, while the lines correspond to the predictions of the QLCA theory. The (Γ, κ) pairs are given in the legend of panel (*b*). Reproduced from [11] (copyright (2008) by IOP Publishing).

is excellent for the $\mathcal{L}$ mode, while some differences in the frequency of the $\mathcal{T}$ waves can be seen in figure 4(*b*). This latter may originate from the less accurate determination of the peak positions of the rather spread $T(k, \omega)$ spectra. Another difference is the cutoff of the $\mathcal{T}$ mode dispersion curve at finite wave numbers. This disappearance of the shear modes for $k \to 0$ is a well-known feature of the liquid state [34, 39]. It is noted that this cutoff is not accounted for by the QLCA, as it does not include damping effects.

5. Transport properties

Molecular dynamics simulations offer two basic ways to study transport processes. In non-equilibrium simulation methods, an external perturbation is applied to the system and the system's response (linked to the perturbation through a transport coefficient) is measured. In equilibrium simulations, time correlation functions of certain microscopic quantities are measured and macroscopic transport coefficients are obtained through the Green–Kubo (GK) relations.

Here, we first review the data available for the transport coefficients of strongly coupled 3D Coulomb and Yukawa OCP. Subsequently, we discuss the transport properties of 2D systems.

5.1. Self-diffusion

The self-diffusion coefficient of the Coulomb OCP as a function of Γ (normalized as $D^* = D/a^2\omega_0$) is displayed in figure 5. Hansen *et al* [34] made use of the GK relation to obtain the self-diffusion coefficient of the Coulomb OCP; their results were found to follow the approximate relation $D^* = 2.95\Gamma^{-1.34}$. Ohta and Hamaguchi [40] obtained the self-diffusion coefficient for Yukawa liquids over a wide domain of the coupling (Γ) and screening (κ) parameters from MD simulations using the mean squared displacement $D = \lim_{t\to\infty} \frac{1}{6t}\langle|\mathbf{r}_i(t) - \mathbf{r}_i(0)|^2\rangle$. Their results for $\kappa = 0.1$ as well as our present data (based on the same computational procedure) obtained for $\kappa = 0$ are also shown in figure 5. These

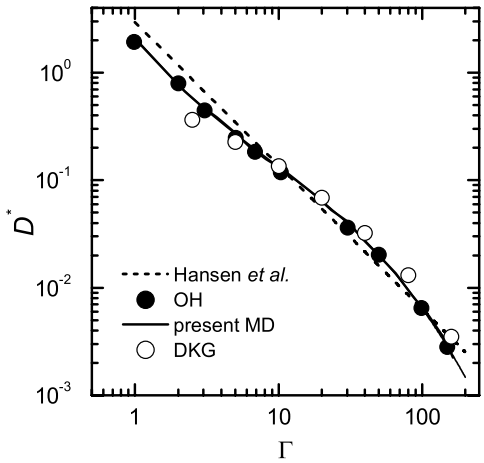

Figure 5. Self-diffusion coefficient of the 3D OCP. Hansen *et al*: [34], OH: Ohta and Hamaguchi [40], DKG: Donkó, Kalman and Golden, calculated from cage correlation functions [12]. The self-diffusion coefficient has been normalized as $D^* = D/a^2\omega_0$. All data correspond to $\kappa = 0$, except OH, which is for $\kappa = 0.1$.

more recent MD data fall very close to those given by the above formula. An additional set of data derived on the basis of the caged behavior and jumping of the particles in the strongly coupled liquid phase [12] is also shown in figure 5. This data set agrees quite well with the results of the 'direct' MD calculations.

5.2. Shear viscosity

Shear viscosity data for the 3D OCP (normalized as $\eta^* = \eta/mna^2\omega_0$) are shown in figure 6. The first data originate from the work of Vieillefosse and Hansen [41]. They have found that η exhibits a minimum at $\Gamma \approx 20$. The calculations of Wallenborn and Baus [42, 43] were based on the kinetic theory; their results were in reasonable agreement with the previous results of [41]. The minimum value of η agreed well for both reports; however, the position of the minimum was reported in [42] to occur at a lower coupling value, $\Gamma \approx 8$. MD simulation was first applied by Bernu *et al* [44, 45] to obtain transport parameters through the GK relations. Donkó and Nyíri [46] used a non-equilibrium MD simulation technique to determine the shear viscosity, while subsequently, Bastea [47] applied equilibrium simulation and obtained η from the GK relation. Daligault [25] has found that the shear viscosity of the OCP follows an Arrhenius-type behavior at high Γ values. Salin and Caillol [19] have carried out equilibrium MD computations for the shear and bulk viscosity coefficients, as well as for the thermal conductivity of the Yukawa OCP. They have implemented Ewald sums for the potentials, the forces and the currents which enter the GK formulae. Saigo and Hamaguchi [48] have also used the GK relations for the calculations of η. A critical review of the shear viscosity calculations of 3D Yukawa liquids and simulations with improved accuracy using two independent nonequilibrium MD methods has been presented in [49].

5.3. Thermal conductivity

Thermal conductivity data for the 3D OCP (normalized as: $\lambda^* = \lambda/nk_Ba^2\omega_0$) are shown in figure 7. Bernu *et al* [44, 45] used the GK relations in conjunction with an equilibrium

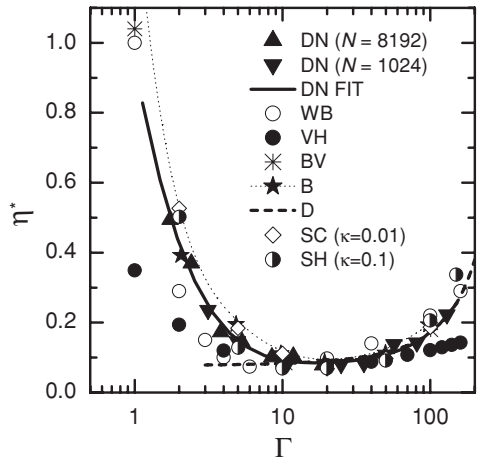

Figure 6. Shear viscosity coefficient of the 3D OCP. DN: Donkó and Nyíri [46] using 1024 and 8192 particles, WB: Wallenborn and Baus [42, 43], VH: Vieillefosse and Hansen [41], BV: Bernu *et al* [44, 45], B: Bastea [47], D: Daligault [25], SC: Salin and Caillol [19], SH: Saigo and Hamaguchi [48]. (The results of [25] have been scaled to match the minimum value of η.) Reproduced from [49] (copyright (2008) by the American Physical Society).

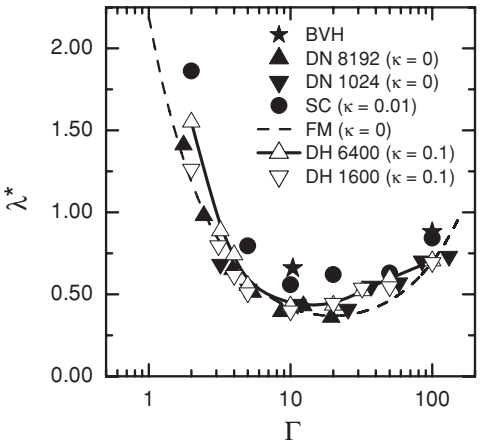

Figure 7. Thermal conductivity coefficient of the 3D OCP. BVH: Bernu *et al* [44, 45], DN: Donkó and Nyíri [46] using 1024 and 8192 particles, SC: Salin and Caillol [19], DH: Donkó and Hartmann [51].

MD simulation to derive λ, while a non-equilibrium MD technique was used in [46, 50]: a perturbation to the system and λ^* was deduced from the relaxation time of the system toward the equilibrium state. Donkó and Hartmann [51] applied the non-equilibrium MD method of [52] to calculate the thermal conductivity of Yukawa liquids. Faussurier and Murillo obtained thermal conductivity (as well as self-diffusion and shear viscosity) values for the Yukawa OCP through its mapping with the Coulomb OCP system, based on the Gibbs–Bogolyubov inequality [53].

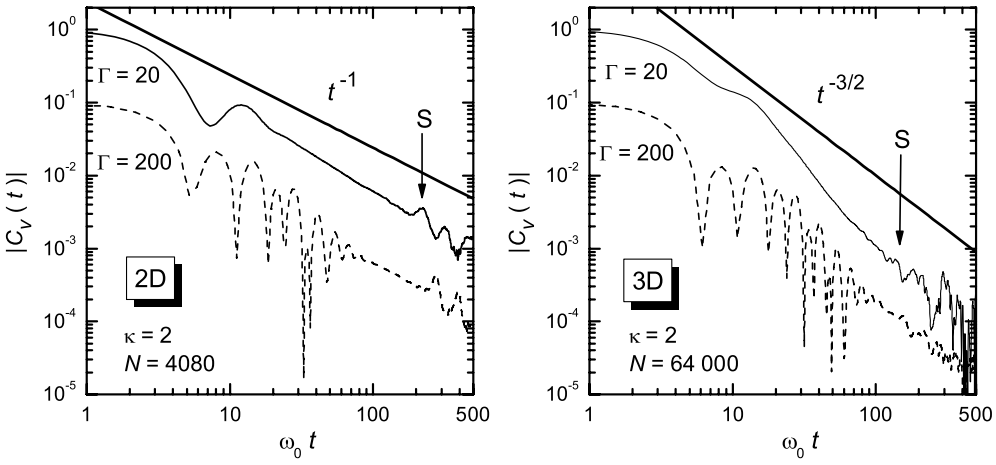

Figure 8. Velocity autocorrelation functions of 2D and 3D Yukawa liquids for the Γ and κ values indicated. The thick lines indicate power-law decays.

We note that the effect of the plasma environment in dusty plasmas has been taken into account in the calculation of transport coefficients of Yukawa systems through Langevin dynamics in several works; see, e.g., [54, 55].

5.4. Transport in two-dimensional systems

The calculation of the transport coefficients through the GK formulae assumes that the integrands appearing in them are integrable. Several previous studies have, on the other hand, demonstrated that this is not always the case. Non-exponential long-time tails in the *velocity autocorrelation function* (VACF) of hard sphere and hard disk systems were first reported in [56]. For the 2D (hard disk) system, the observed t^{-1} decay of the VACF evidently precludes the use of the GK relation to compute D. (For 3D, a $t^{-3/2}$ decay was predicted in [56].) Ever since this observation, the existence of transport coefficients in 2D systems has been a topic of controversy. For 2D systems, a t^{-1} long-time decay (similar to that of the VACF) was predicted by theory [57] also both for the *stress autocorrelation function* (SACF) and the *energy current autocorrelation function* (EACF). 2D soft disk fluid simulations have confirmed the t^{-1} tail of the SACF [58]. For certain conditions, superdiffusion was also observed in 2D Yukawa systems [59]. A transition between superdiffusion and 'normal' diffusion has been found to take place as controlled by the thickness of a quasi-2D layer in a simulation of a system confined in one direction [60].

Figure 8 presents VACFs obtained from MD simulations of 2D and 3D Yukawa liquids, for different values of Γ. At high coupling (Γ = 200), the curves exhibit initial oscillations due to caged particle oscillations; subsequently, we observe a part with smooth decay. Since the curves are presented using log–log scales, a straight line corresponds to a power-law decay. The meaningful length of data is limited by the finite size of the simulation box; following the smoothly decaying parts of the curves as spurious features, we observe peaks (the first of them labeled as 'S' in the graphs) originating from the traverse of sound waves through the simulation boxes. At high coupling, in the case of a 2D system we observe a closely t^{-1} long-time decay of the VACF and a closely $t^{-3/2}$ decay in the case of 3D. The t^{-1} decay suggests that the VACF is non-integrable and consequently the diffusion coefficient does not exist. At the lower value of coupling the VACFs decay faster, allowing for a meaningful

D to exist even in 2D. Clarification of the behavior of the shear stress and energy current autocorrelation functions of 2D Yukawa systems is a topic of current work [61].

6. Summary

This paper intended to illustrate the application of molecular dynamics simulations in the exploration of the physics of strongly coupled plasmas. After having discussed the basic characteristics of SCPs and the essentials of the molecular dynamics simulations, MD results have been shown for the structural and dynamical characteristics as well as for transport coefficients of 3D Coulomb and Yukawa systems. Issues related to the existence of phases and transport coefficients in 2D systems have been discussed. Clarification of some of these issues requires a significant increase of computer power; these large-scale simulations remain for future work.

Acknowledgments

The author wishes to acknowledge fruitful collaboration on the topics presented here, with G J Kalman, P Hartmann, K I Golden, K Kutasi, J Goree, M Rosenberg, S Kyrkos, M Bonitz and T Ott. This work has been supported by the Hungarian Fund for Scientific Research OTKA-T048389, OTKA-PD75113, OTKA-IN69892 and by a bilateral grant between the Hungarian Academy of Sciences and the National Science Foundation of USA (MTA/NFS-102).

References

[1] Kalman G J, Rommel J M and Blagoev K 1998 *Strongly Coupled Coulomb Systems* (New York: Plenum)
2003 *J. Phys. A: Math. Gen.* **36** (special issue)
2006 *J. Phys. A: Math. Gen.* **39** (special issue)
[2] Grimes C C and Adams G 1976 *Phys. Rev. Lett.* **36** 145
[3] Glattli D C, Andrei E Y and Williams F I B 1988 *Phys. Rev. Lett.* **60** 420
[4] Hansen J-P, Torrie G and Vieillefosse P 1977 *Phys. Rev.* A **16** 2153
[5] Iyetomi H, Ogata S and Ichimaru S 1989 *Phys. Rev.* B **40** 309
[6] Melzer A, Schweigert V A, Schweigert I V, Homann A, Peters A and Piel A 1996 *Phys. Rev.* E **54** R46
Zuzic M, Ivlev A V and Goree J *et al* 2000 *Phys. Rev. Lett.* **85** 4064
Robertson S, Gulbis A A S, Collwell J and Horányi M 2003 *Phys. Plasmas* **10** 3874
Sternovsky Z, Lampe M and Robertson S 2004 *IEEE Trans. Plasma Sci.* **32** 632
Fortov V E, Ivlev A V, Khrapak S A, Khrapaka A G and Morfill G E 2005 *Phys. Rep.* **421** 1
[7] Kainth D S, Richards D, Richards H P, Simmons M Y and Ritchie D A 2000 *J. Phys.: Condens. Matter* **12** 439
[8] Mitchell T B, Bollinger J J, Dubin D H E, Huang X-P, Itano W M and Baughman R H 1998 *Science* **282** 1290
[9] Matthews L S, Qiao K and Hyde T W 2006 *Adv. Space Res.* **38** 2564
Smith B, Hyde T, Matthews L, Reay J, Cook M and Schmoke J 2008 *Adv. Space Res.* **41** 1509
[10] Arp O, Block D and Piel A 2004 *Phys. Rev. Lett.* **93** 165004
Sheridan T E 2007 *Phys. Plasmas* **14** 032108
Kong M, Partoens B and Peeters F M 2003 *New J. Phys.* **5** 23
Bonitz M, Block D and Arp O *et al* 2006 *Phys. Rev. Lett.* **96** 075001
[11] Donkó Z, Kalman G J and Hartmann P 2008 *J. Phys.: Condens. Matter* **20** 413101
[12] Donkó Z, Kalman G J and Golden K I 2002 *Phys. Rev. Lett.* **88** 225001
Donkó Z, Hartmann P and Kalman G J 2003 *Phys. Plasmas* **10** 1563
[13] Streitz F *et al* 2008 Particle simulations of hot dense matter with radiation *SCCS2008 Book of Abstracts* p 62
[14] Frenkel D and Smit B 1996 *Understanding Molecular Simulation* (San Diego, CA: Academic)
[15] Baimbetov F B, Ramazanov T S, Dzhumagulova K N, Kadyrsizov E R, Petrov O F and Gavrikov A V 2006 *J. Phys. A: Math. Gen.* **39** 4521
[16] Ewald P P 1921 *Ann. Phys.* **64** 253
[17] Eastwood J W, Hockney R W and Lawrence D N 1980 *Comput. Phys. Commun.* **19** 215
Hockney R and Eastwood J 1981 *Computer Simulation Using Particles* (New York: McGraw-Hill)

[18] Sagui C and Darden T A 1999 *Ann. Rev. Biophys. Biomol. Struct.* **28** 155
[19] Salin G and Caillol J-M 2002 *Phys. Rev. Lett.* **88** 065002
Salin G and Caillol J-M 2003 *Phys. Plasmas* **10** 1220
[20] Johnson R E and Ranganathan S 2001 *Phys. Rev.* E **63** 056703
[21] Farouki R T and Hamaguchi S 1993 *Phys. Rev.* E **47** 4330
[22] Stringfellow G S, DeWitt H E and Slattery W L 1990 *Phys. Rev.* A **41** 1105
[23] Hamaguchi S, Farouki R T and Dubin D H E 1997 *Phys. Rev.* E **56** 4671
[24] McQuarrie D 2000 *Statistical Mechanics* (Sausalito, CA: Univ. Sci. Books)
[25] Daligault J 2006 *Phys. Rev. Lett.* **96** 065003
[26] Peierls R E 1935 *Ann. Inst. Henri Poincaré* **5** 177
Landau L D 1937 *Phys. Z. Sovjet.* **11** 26
Hohenberg P C 1966 *Phys. Rev.* **158** 383
Mermin N D 1968 *Phys. Rev.* **176** 250
[27] Hartmann P, Donkó Z, Bakshi P, Kalman G J and Kyrkos S 2007 *IEEE Trans. Plasma Sci.* **35** 332
[28] Gann R C, Chakravarty S and Chester G V 1979 *Phys. Rev.* B **20** 326
[29] Halperin B I and Nelson D R 1978 *Phys. Rev. Lett.* **41** 121
[30] Kosterlitz J M and Thouless D J 1973 *J. Phys. C: Solid State Phys.* **6** 1181
[31] Chui S T 1982 *Phys. Rev. Lett.* **48** 933
Aeppli G and Bruinsma R 1984 *Phys. Rev. Lett.* **53** 2133
Strandburg K J 1988 *Rev. Mod. Phys.* **60** 161
Simon Ch, Rosenman I, Batallan F, Lartigue C and Legrand J F 1992 *Phys. Rev.* B **45** 2694
Ryzhov V N and Tareyeva E E 1995 *Phys. Rev.* B **51** 8789
[32] Ogawa T, Totsuji H, Totsuji C and Tsuruta K 2006 *J. Phys. Soc. Japan.* **75** 123501
[33] Böning J, Filinov A, Ludwig P, Baumgartner H, Bonitz M and Lozovik Yu E 2008 *Phys. Rev. Lett.* **100** 113401
[34] Hansen J P, McDonald I R and Pollock E L 1975 *Phys. Rev.* A **11** 1025
[35] Ohta H and Hamaguchi S 2000 *Phys. Rev. Lett.* **84** 6026
[36] Hamaguchi S and Ohta H 2000 *J. Phys. IV France* **10** Pr5–19
[37] Hartmann P, Kalman G J, Donkó Z and Kutasi K 2005 *Phys. Rev.* E **72** 026409
[38] Kalman G J, Rosenberg M and DeWitt H E 2000 *Phys. Rev. Lett.* **84** 6030
[39] Totsuji H and Kakeya N 1980 *Phys. Rev.* A **22** 1220
Schmidt P, Zwicknagel G, Reinhard P-G and Toepffer C 1997 *Phys. Rev.* E **56** 7310
Murillo M S 2000 *Phys. Rev. Lett.* **85** 2514
[40] Ohta H and Hamaguchi S 2000 *Phys. Plasmas* **7** 4506
[41] Vieillefosse P and Hansen J-P 1975 *Phys. Rev.* A **12** 1106
[42] Wallenborn J and Baus M 1977 *Phys. Lett.* A **61** 35
[43] Wallenborn J and Baus M 1978 *Phys. Rev.* A **18** 1737
[44] Bernu B, Vieillefosse P and Hansen J-P 1977 *Phys. Lett.* A **63** 301
[45] Bernu B and Vieillefosse P 1978 *Phys. Rev.* A **18** 2345
[46] Donkó Z and Nyíri B 2000 *Phys. Plasmas* **7** 45
[47] Bastea S 2005 *Phys. Rev.* E **71** 056405
[48] Saigo T and Hamaguchi S 2002 *Phys. Plasmas* **9** 1210
[49] Donkó Z and Hartmann P 2004 *Phys. Rev.* E **78** 026408
[50] Donkó Z, Nyíri B, Szalai L and Holló S 1998 *Phys. Rev. Lett.* **81** 1622
[51] Donkó Z and Hartmann P 2004 *Phys. Rev.* E **69** 016405
[52] Müller-Plathe F 1997 *J. Chem. Phys.* **106** 6082
[53] Faussurier G and Murillo M S 2003 *Phys. Rev.* E **67** 046404
[54] Vaulina O S and Vladimirov S V 2002 *Phys. Plasmas* **9** 835
Vaulina O S and Dranzhevskii I E 2007 *Plasma Phys. Rep.* **33** 494
[55] Dzhumagulova K and Ramazanov T 2006 *Abstract Book of the 12th Int. Workshop on the Physics of Non-Ideal Plasmas (Darmstadt, Germany, 4–8 Sep.)* P07
[56] Alder B J and Wainwright T E 1970 *Phys. Rev.* A **1** 18
[57] Ernst M H, Hauge E H and van Leeuwen J M J 1970 *Phys. Rev. Lett.* **25** 1254
[58] Morriss G P and Evans D J 1985 *Phys. Rev.* A **32** 2425
[59] Liu B and Goree J 2007 *Phys. Rev.* E **75** 016405
Liu B and Goree J 2008 *Phys. Rev. Lett.* **100** 055003
[60] Ott T, Donkó Z, Hartmann P and Bonitz M 2008 *Phys. Rev.* E **78** 026409
[61] Donkó Z, Goree J, Hartmann P and Liu B 2008 in preparation